Precision Engineering 43 (2016) 486–492

Contents lists available at ScienceDirect

Precision Engineering

journal homepage: www.elsevier.com/locate/precision

Diagonal in space of coordinate measuring machine verification using an optical-comb pulsed interferometer with a ball-lens target

Wiroj Sudatham [a,*], Hirokazu Matsumoto [a], Satoru Takahashi [b], Kiyoshi Takamasu [a]

[a] Department of Precision Engineering, The University of Tokyo, Hongo 7-3-1, Bunkyo-ku, Tokyo 113-8656, Japan
[b] Research Center for Advanced Science and Technology, The University of Tokyo, Komaba 4-6-1, Meguro, Tokyo 153-8904, Japan

ARTICLE INFO

Article history:
Received 30 July 2015
Received in revised form 9 September 2015
Accepted 16 September 2015
Available online 30 September 2015

Keywords:
Optical comb
Pulsed interferometer
Length measurement
Coordinate measuring machine
CMM verification

ABSTRACT

This paper presents a new optical method of coordinate measuring machine (CMM) verification. The proposed system based on a single-mode fiber optical-comb pulsed interferometer with a ball lens of refractive index 2 employed as the target. The target can be used for absolute-length measurements in all directions. The laser source is an optical frequency comb, whose repetition rate is stabilized by a rubidium frequency standard. The measurement range is confirmed to be up to 10 m. The diagonals of a CMM are easier to verify by the proposed method than by the conventional artifact test method. The measurement uncertainty of the proposed method is also smaller than that of the conventional method because the proposed measurement system is less affected by air temperature; it achieves an uncertainty of approximately 7 μm for measuring lengths of 10 m. The experimental results show that the measurement accuracy depends on noise in the interference fringe, which arises from airflow fluctuations and mechanical vibrations.

1. Introduction

Coordinate measuring machines (CMMs) are widely used to measure the three-dimensional sizes, forms, and positions of workpieces. Demonstrating traceability to the International System of Units (SI) and estimating the accuracy of CMM measurements are critical to maintaining confidence in their reliability. Therefore, CMMs must be calibrated upon installation and verified periodically during operation. The main tests required to decide whether the CMM performs to the maximum permissible error of length measurement specified by the manufacturer are detailed in Part 2 of the International Organization for Standardization (ISO) 10360 series [1]. The standard states that five different lengths should be chosen. The longest calibrated test length should be at least 66% of the maximum travel of the CMM. Measurements should be performed in four required positions along the space diagonals shown in Fig. 1, and in three positions parallel to each of the CMM axes. Many methods using calibration artifacts and continuous wave (CW) laser interferometers have been developed to verify CMMs [1–11].

Most methods prefer to use end standards, such as a series of gauge blocks, a step gauge, or a ball plate. However, evaluating large-CMMs (measuring volumes over 2 m^3) has been problematic because of the unavailability of large calibration artifacts. Large calibrated artifacts are difficult to produce because of their size and weight. Calibrating large gauges is difficult, and maintaining gauge accuracy during storage and handling is troublesome [12,13]. Although a CW-laser interferometer can measure long lengths along body diagonals, the measurements can be slow and require difficult laser beam alignment. Moreover, the measurement path cannot be interrupted during the measurement period, because it is operated based on interference fringe counting method.

Recently, optical frequency combs have been proven useful tools for dimensional metrology because of their high frequency-stability and direct traceability to the SI base unit [14]. Several length measurement methods using optical frequency combs have been proposed [15–19]. We developed an optical system for large-size CMM verification that overcomes the problems of conventional artifact test methods. The new system is based on a single-mode fiber optical-comb pulsed interferometer, and uses a ball lens of refractive index 2 as a target. The repetition frequency of a general optical comb is generated, and an optical fiber etalon (Fabry-Pérot fiber etalon) is used as a frequency mode selector to generate interference fringes at the required absolute positions. The performance of long-range measurements was demonstrated by preliminary absolute-length measurements. The proposed system can be used to measure absolute length up to 10 m. The proposed system was used to verify the diagonals of a moving-bridge type CMM in

* Corresponding author. Tel.: +81 3 5841 6472; fax: +81 3 5841 6472.
E-mail address: wiroj@nanolab.t.u-tokyo.ac.jp (W. Sudatham).

http://dx.doi.org/10.1016/j.precisioneng.2015.09.017
0141-6359/

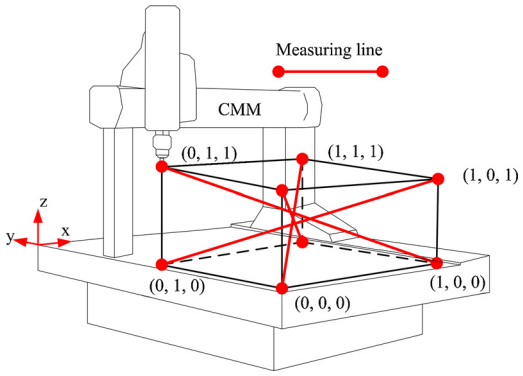

Fig. 1. Measuring lines of the diagonals in space of a CMM; opposite corners of the measuring volume are assumed to be (0, 0, 0) and (1, 1, 1) in coordinates (*X*, *Y*, *Z*).

volume space, as was an artifact test method, for comparison, and the measurement uncertainties of both techniques are discussed.

2. Principle of measurement

The proposed measurement technique is based on a single-mode fiber interferometer, as shown in Fig. 2. An optical comb (C-Fiber femtosecond laser, MenloSystems) with a 1560 nm central wavelength and a 100 MHz repetition frequency stabilized by a rubidium frequency standard generates a laser pulse that passes through a fiber etalon with a free spectral range (FSR) of 1 GHz. An optical amplifier amplifies the laser beam, which then passes through an optical fiber circulator (CIR) to a fiber beam splitter (FBS). One of the resulting split beams is collimated by a collimator (C1) toward a scanning mirror (M1), while the other is collimated by a lens, transmitted through a sapphire window plate (SW) at the reference position before reaching probing target. This second beam acts as measurement arms of a Michelson interferometer.

Subsequently, the beams reflected from the SW at the reference position and the target recombine with the beam reflected from the scanning mirror M1 to generate interference fringes when the optical path differences (*OPD*) between the two arms follow Eq. (1) [16,17].

$$OPD = \frac{mc}{n_{air} f_{rep}} \tag{1}$$

where m is an integer, c is the speed of light in the vacuum, n_{air} is the group refractive index of air [20,21], and f_{rep} is the repetition frequency. The interference fringe signals return to the output port of the CIR and are subsequently detected by a photodetector (2053FC-M, Newport), and observed by an oscilloscope.

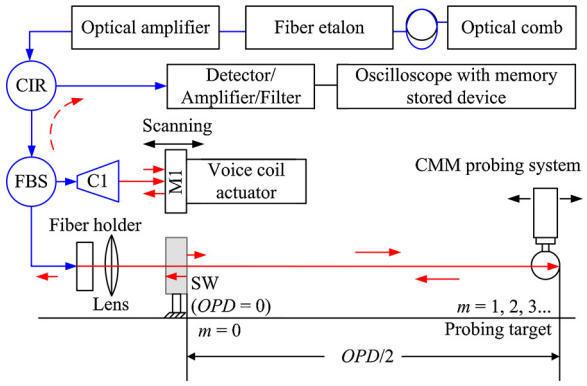

Fig. 2. Diagram of the proposed measurement system; CIR is an optical fiber circulator, FBS is a fiber beam splitter, C1 is a collimator, and SW is a sapphire window plate (reference position). The optical components are connected by optical fibers.

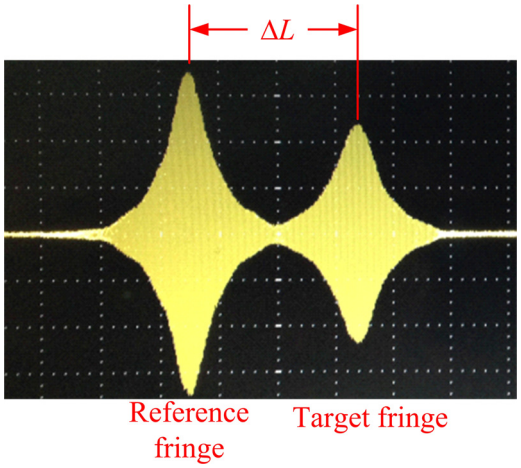

Fig. 3. Interference fringes; the first fringe is produced by reflection of the SW at the reference position. The second is generated by the target.

Two interference fringes overlap with each other when the *OPD* exactly satisfy Eq. (1). In practice, if the measurement length provides a displacement ΔL, the envelope interference fringes will be separated, as shown in Fig. 3.

Therefore, the absolute measurement length is determined by Eq. (2), where ΔL is the distance between the peaks of the interference fringe envelopes.

$$L = \frac{mc}{2n_{air} f_{rep}} + \Delta L \tag{2}$$

The interference fringes of a pulsed interferometer, as shown in Fig. 3, are represented in the time domain. The time scale must be converted to a length scale to determine the distance between the peaks of the interference fringe envelopes, ΔL [18].

3. Experiments and results

3.1. Pulsed interferometer accuracy

The accuracy of the proposed pulsed interferometer was directly evaluated using a standard length of long gauge block. The measurement setup is shown in Fig. 4.

A long gauge block [LGB, 150 mm, grade-0, thermal expansion coefficient $(10.8 \pm 0.5) \times 10^{-6}\ K^{-1}$] was used as the standard length. The first facet of the LGB was wrung by an optical parallel, and the other was wrung by a short gauge block (GB). The Airy points of the LGB were supported by two pin gauges on a translation stage. The optical components were as described in Fig. 2; the laser beam of an optical comb passed through a fiber etalon and was aligned perpendicular to the optical parallel plate over the travel length of the translation stage. The translation stage was moved until the first interference fringe appeared due to the beam reflected from the inner surface of the optical parallel. The second fringe will automatically arise from the facet of the GB due to the traveling stroke of the scanning device expending the length of the *OPD*. A temperature sensor was attached to the LGB, and a metal sheet covered the measurement setup for more than 24 h to stabilize the temperature of the LGB before measurements were taken. The averages of 10 repeated measurements are shown in Table 1.

The measurements in Table 1 indicate sufficient accuracy of the optical-comb pulsed interferometer for CMM verification.

The precise positions of the interference fringes are very significant to the accuracy of pulsed interferometer, which is used to determine the absolute-length measurement. It relates to the FSR of the fiber etalon, which is proportional to the refractive index of the fiber medium and the length of the fiber cavity. Fabricating a

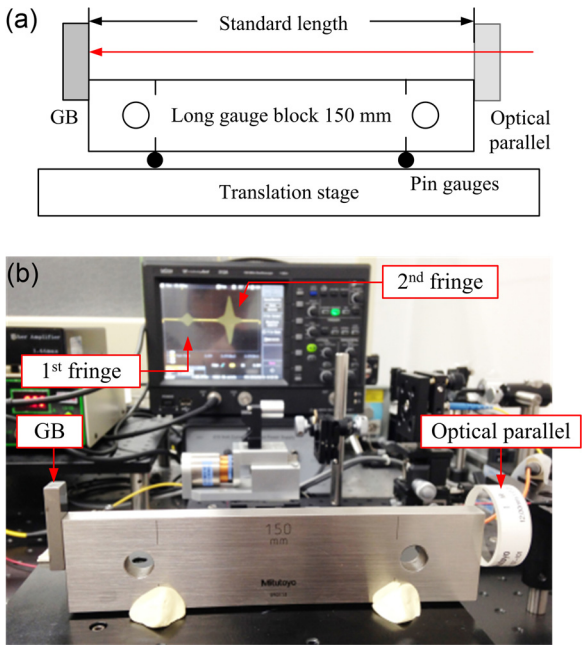

Fig. 4. Measurement comparing the position of interference fringes with a standard length 150 mm long gauge block. (a) Diagram of measurement setup. (b) Photograph of the experimental setup.

Table 1
Accuracy of pulsed interferometer determined by comparison with the length of a standard gauge block.

	T_{LGB} (°C)	ΔL_t (mm)	LGB_t (mm)	Measured value (mm)	Difference (μm)
Average	21.82	0.00294	150.00294	150.00301	−0.07
SD	0.01	0.00002	0.00002	0.00009	–
Variation	0.03	0.00005	0.00005	0.00027	–

T_{LGB} is the gauging temperature of the long gauge block. ΔL_t is the length of thermal expansion. LGB_t is the actual length of the long gauge block at the average temperature of 21.82 °C, and SD is the measurement standard deviation.

preface fiber etalon is difficult because of the inhomogeneous-medium indices of the fiber and coating etalon. The etalon cavity length is also difficult to control, and so must be measured and compensated. The FSR is related to the full-width half-maximum of any one transmission band by a quantity known as the finesse; high finesse fiber etalons are required for this application as they show sharper transmission peaks with lower minimum transmission coefficients [22].

3.2. Ball lens target

We aimed to develop a system that can observe interference fringes in all measurement directions. Therefore, a ball lens (S-LAH79, Ohara) with a refractive index of 2 and a diameter of 10 mm was used as the target of our pulsed interferometer. The back focal length of the ball lens was set to zero. When this ball lens is employed as a target, the entire incoming beam will focus at the ball-lens end surface, as shown in Fig. 5. The reflected beam retraces its incoming path in the opposite direction. Thus, the ball lens functions as a retroreflector [23,24].

The total accuracy of the ball lens target depends on the accuracies of both the refractive index of glass material and the spherical fabrication. The following experiment demonstrates the simplest method to determine the contribution of a ball lens target to optical path error, as shown in Fig. 6.

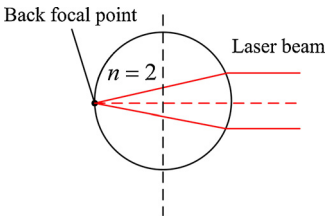

Fig. 5. Structure diagram of the ball-lens target.

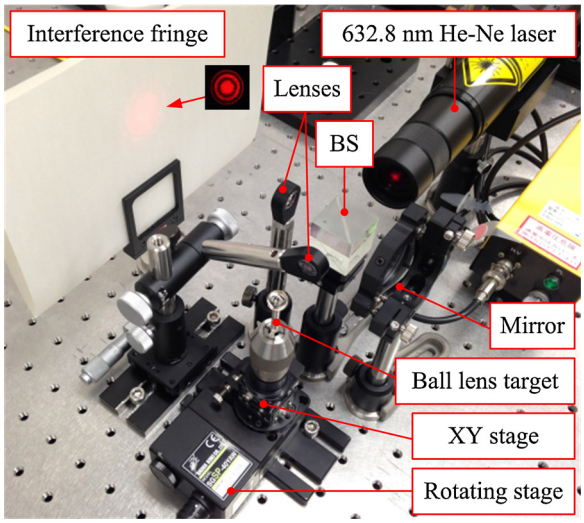

Fig. 6. Experimental setup of method determining the effect of a ball lens target on optical path error.

The experimental setup is based on a general unbalanced-arm Michelson interferometer. A long-coherence light source (632.8 nm He-Ne laser, NEOARK) served as a light source. The laser beam was divided by a beam splitter. One beam was collimated by a lens to the back focal point of a ball lens target, and the other was incident on the reference mirror. The beams reflected from the target and the reference mirror recombined to produce a pattern fringe on an imaging screen. The ball lens was positioned to be concentric with a translation stage to avoid errors of stage rotation. The laser beam was then aligned until a fringe pattern appeared. The ball lens was rotated by the rotating stage, and the pattern fringe on the screen was observed.

In observation, the pattern fringe did not change during ball lens rotation. It can be implied that the ball lens caused an optical path error of less than one half of the laser source wavelength, i.e., less than 0.3 μm. However, vibration of the rotating stage directly affects the fringe pattern. Therefore, a precise, smoothly rotary stage is required to achieve high precision in the observed fringe pattern. A highly accurate roundness measuring machine to confirm the roundness accuracy of the target is an alternative. However, for one-dimensional length measurements, the sphericity of the ball lens does not affect the optical path difference, but it does significantly affect three-dimensional lengths measurements by the target. Thus, the error due to the target can be ignored for CMM diagonal measurements by the proposed method.

3.3. Preliminary absolute-length measurement

We demonstrated measurement reproducibility of our method by preliminary absolute-length measurements, as shown in Fig. 7. The optical components of this experiment were the same as described in Fig. 2. The absolute-length measurements were made

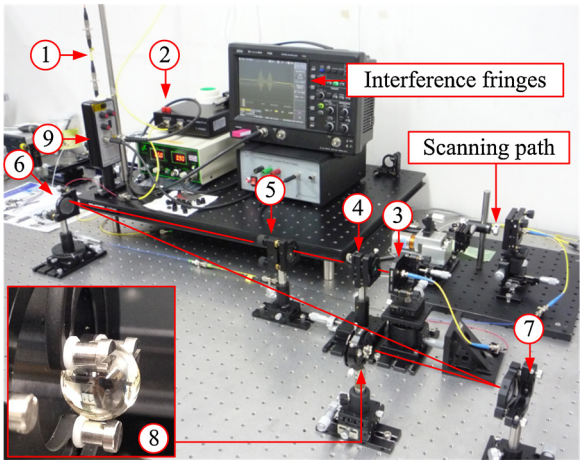

Fig. 7. Preliminary absolute-length measurement set up; (1) is a fiber etalon with 1-GHz FSR, (2) is an optical amplifier, (3) is a fiber holder, (4) is a lens, (5) is a reference position, (6) and (7) are mirrors, (8) is a ball lens target, and (9) is a photodetector.

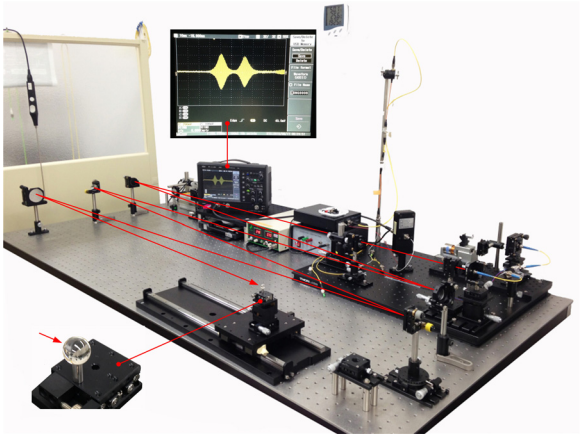

Fig. 8. Long-range measurement of a pulsed interferometer with a ball lens target (absolute-length measurement is approximately 9 m).

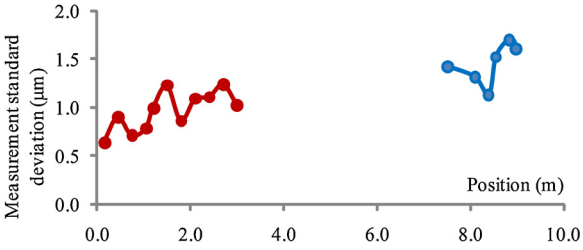

Fig. 9. Preliminary absolute-length measurement results; the maximum measurement standard deviation is approximately 1.25 μm for the measurement range of (0–3) m and 1.71 μm for the measurement range of (7.5–9.0) m.

at target positions approximately every 150 mm up to 3 m. The absolute lengths were measured and determined using Eq. (2).

Finally, we considered the efficiency of the optical-comb pulsed interferometer with the ball lens target in long-range measurements. The measurement setup is similar to the previous experiment, but the target was positioned from 7.5 m to 9.0 m. The measurement setup is shown in Fig. 8, and the measurement results of both the short-range (0–3 m) and long-range (7.5–9.0 m) measurements are shown in Fig. 9.

The maximum measurement standard deviation is approximately 1.25 μm for measurements in the range of (0–3) m, and 1.71 μm for measurements in the range of (7.5–9.0) m. The

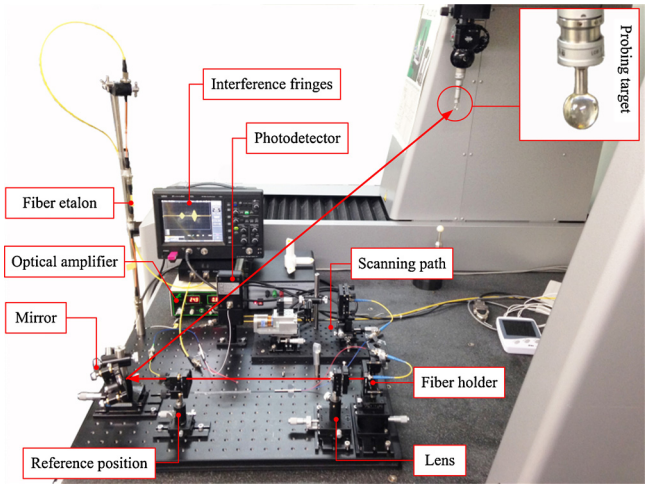

Fig. 10. Space diagonal of a CMM measurement using the pulsed interferometer.

reproducibility is mainly affected by environmental conditions, especially airflow fluctuations and mechanical vibrations. However, the interference fringes at 9.0 m are very clear, as illustrated in Fig. 8. These pattern fringes show that the signal-to-noise ratios of the long length measurements are very high. Therefore, the experimental results strongly indicate that the proposed measurement system can measure absolute lengths for a range of applications, because the maximum measurement volumes of most large-CMMs are approximately 10 m^3.

3.4. CMM space diagonals verification

A compact pulsed interferometer was connected to an optical comb passing through an optical fiber over 100 m from the 10th floor to the basement floor of a building. (The optical comb was installed at the 10th floor, and the CMM was installed at the basement of the building). A ball lens target was fixed on a CMM probe head. The diagonals of a moving bridge-type CMM (FALCIO APEX 707, Mitutoyo) were measured by the proposed technique, as shown in Fig. 10. First, the measurement lines were defined as in Fig. 1. To avoid optical path error due to the different refractive indices of air and the target, the initial zero positions of both the CMM and interferometer were set for a value of $m \geq 1$; therefore, the initial positions would compensate for the optical path error of each position. Absolute length measurements of the CMM probe were made at 150 mm increments along its diagonals using the proposed system.

To confirm the efficiency of our proposed method, these measurements were compared with the results of a standard artifact test method. The artifact was a step-gauge (S232, KOBA-step) with a steel frame, 16 ceramic gauges, 32 faces, and 20 mm nominal length. The thermal expansion coefficient was 11.5×10^{-6} K^{-1}. This step gauge was supported, and the reference lengths were measured by the National Metrology Institute of Japan, (NMIJ). The step gauge was aligned to approximate the measurement lines of the proposed method along the four diagonals of the CMM. A temperature sensor was attached to the gauge to monitor the gauge temperature during measurements. Each measurement line was measured only after the temperature of the step gauge had remained stable for more than 3 h. The diagonals of the CMM were verified, and the measurement results were corrected to the reference temperature (20 °C) [25]. The results of both methods are shown in Fig. 11(a)–(d), where the blue-diamonds lines are indication error of a CMM that measured by the proposed system, the red-circles lines are measured by a step gauge method, and

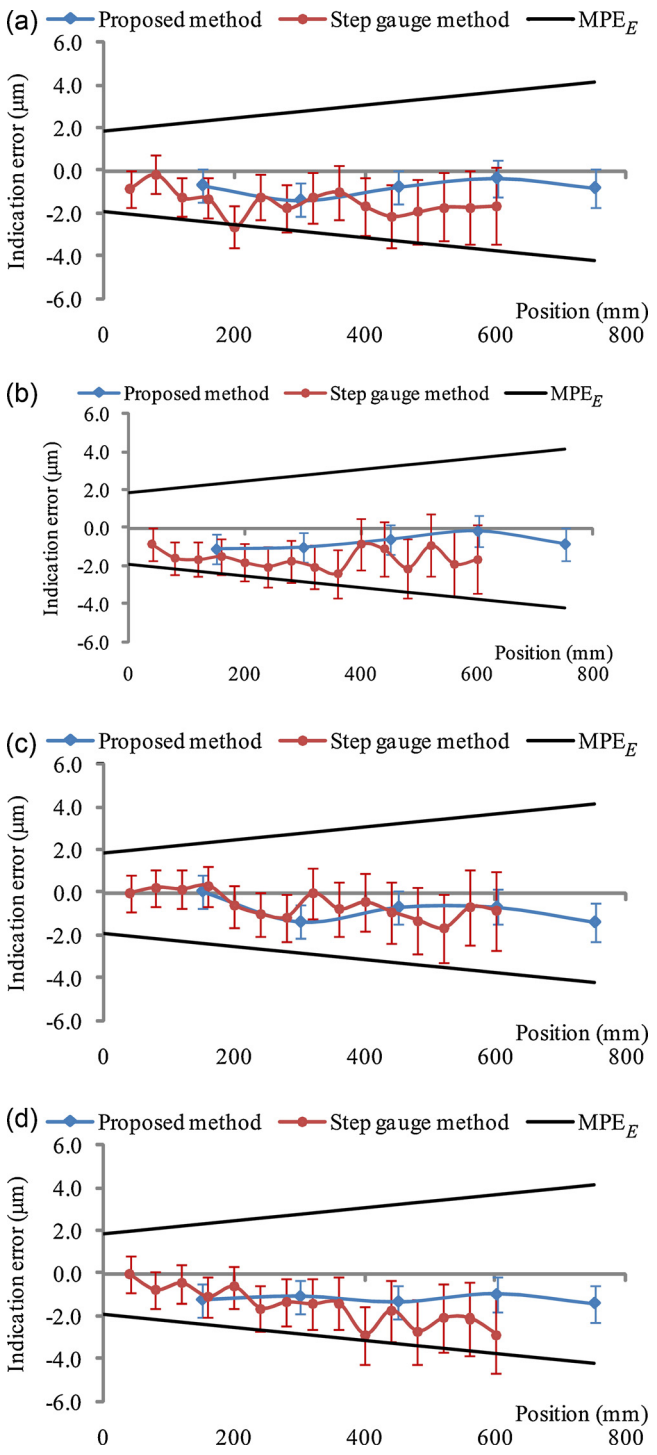

Fig. 11. Comparison of indication errors of CMM diagonal lines measured by the proposed method (blue diamonds), a standard step gauge method (red circles). MPE$_E$ is the maximum permissible error. (For interpretation of the references to color in this figure legend, the reader is referred to the web version of this article.)

the black lines are the maximum permissible error of a CMM. The measurements along the diagonal in space of a CMM refer to Fig. 1.

In the measurement comparisons, to reduce probing error of the CMM, only unidirectional measurements of step gauge were considered. The results show that all position measurements fall within the maximum permissible error of indication of a CMM for size measurement [MPE$_E$ = ±(1.9 + 3l/1000) μm, where l is the indication length of the CMM measurement in mm]. The differences between the uncertainties of measurements are discussed in the next section. However, the proposed method is non-contact, and the positioning accuracy along each diagonal was verified approximately every 150 mm. In contrast, the step gauge methods are contact measurements, and each diagonal was verified at approximately every 40 mm, according to the nominal length of a step gauge. In addition, although error due to stylus tip compensation was eliminated by taking only unidirectional measurements, probing errors of the CMM still affect measurement repeatability. Measurement uncertainty of the proposed method was smaller than that of the step gauge due to slight effects of air temperature, because temperature distribution on a step gauge significantly affects the measurement uncertainty. In addition, the step gauge method is more time consuming than the proposed method because of the wait for stabilized temperature. The proposed method can directly verify a CMM after a 30-min warm up of the measurement system.

4. Uncertainty of measurement

The measurement uncertainty by our proposed method was evaluated in accordance with GUM [26]. The positioning error of each diagonal of the CMM (E_x), as measured by an optical-comb pulsed interferometer, is determined by Eq. (3).

$$E_x = l_x - l_s + \delta l_{ix} + l_N \cdot \alpha \cdot \Delta T \tag{3}$$

where l_x is the indication length of a CMM, l_s is the standard length determined by the proposed method, δl_{ix} is the correction due to finite resolution of the CMM, l_N is the nominal length, α is the thermal expansion coefficient of a linear scale of CMM, ΔT is the difference between the linear scale temperature of a CMM and the reference temperature.

According to Eq. (3), the uncertainty of CMM diagonal measurements is evaluated as Eq. (4).

$$u^2(E_x) = u^2(l_x) + u^2(l_s) + u^2(\delta l_{ix}) + l_N \cdot \Delta T u^2(\alpha) \tag{4}$$

The standard length (l_s), determined as in Eq. (2), relates to the uncertainties of the repetition frequency, the group refractive index of air, and the distance between peaks of the envelope interference fringes. The stability of the repetition frequency after passing through a fiber etalon is in the order of 10^{-9} over 2 h [16]. This partially contributes a length uncertainty of 0.5×10^{-9} l divided by the rectangular distribution, because of the semi-range limits of the finite resolution of the instrument. The uncertainty of the repetition rate and carrier offset frequency of the optical comb are neglected because they are more than 100 times more accurate than the maximum permissible error of a CMM. The standard length was compensated for the group refractive index of air by Ciddor's equation. Therefore, this group refractive index of air equation relates to the uncertainties of air pressure, air humidity, and air temperature. The combined standard uncertainty for the length correction is determined by applying Ciddor's equation, in which the sensitivity coefficients are evaluated by first performing partial derivatives. The contribution to uncertainty of each parameter is evaluated by multiplying standard uncertainties with their sensitivity coefficients [26,27]. The uncertainties due to air pressure, air temperature, and air humidity were evaluated from the maximum variations in the laboratory during measurements; these were 0.1 kPa, 0.40 °C, and 0.5%RH respectively. These parameters were estimated to have rectangular limits, and the uncertainty of Ciddor's equation was estimated to be on the order of 10^{-8}.

Next, the uncertainty in the distance between peaks of interference fringe envelopes was determined by the relationship between time scale and length scale [18]. This was evaluated using the maximum deviation between the measured values and the best-fit line, and assumed to be a rectangular distribution.

Table 2
Uncertainty sources of CMM space diagonal verification using a pulsed interferometer.

Uncertainty source, x_i	Uncertainty value, $u(x_i)$	Uncertainty contribution, $u(y)$
Absolute uncertainty		
Repeatability of measurement	0.18 μm	0.18 μm
Variations due to the finite resolution of a CMM	0.29 μm	0.29 μm
Time and length scale measurement	0.18 μm	0.18 μm
Relative uncertainty		
Stability of modified repetition frequency	$<10^{-9}$	$2.89 \times 10^{-9}\ l$
Ciddor's equation	$<10^{-8}$	$1.00 \times 10^{-8}\ l$
Variation of air humidity	0.29%RH	$2.95 \times 10^{-9}\ l$
Variation of air pressure	57.74 Pa	$1.52 \times 10^{-7}\ l$
Variation of air temperature	0.23 °C	$2.11 \times 10^{-7}\ l$
Thermal expansion coefficient	1×10^{-6} K^{-1}	$2.31 \times 10^{-7}\ l$
Combined standard uncertainty	$[(0.38\ \mu m)^2 + (3.48 \times 10^{-7} l)^2]^{1/2}$	

l is the indication length of a CMM in mm.

Table 3
Uncertainty sources of CMM diagonal verification using a step gauge.

Uncertainty source, x_i	Uncertainty contribution, $u(y)$	
	Absolute	Relative
Uncertainty of step gauge	0.09 μm	$2.40 \times 10^{-7}\ l$
Repeatability of measurement	0.32 μm	–
Variations due to the finite resolution of a CMM	0.29 μm	–
Correction due to temperature distribution	–	$1.41 \times 10^{-6}\ l$
Expanded uncertainty $[(0.87)^2 + (2.86 \times 10^{-3} l)^2]^{1/2}$ μm		

l is the indication length of a CMM in mm.

In the measurement, the difference in temperature between linear scale of a CMM and a reference temperature cannot be directly measured, and the positions of a CMM in each diagonal were automatically corrected for thermal expansion to the reference temperature by CMM's software. Therefore, only uncertainty of the thermal expansion coefficient was considered.

The digital scale interval of the linear scale of CMM is 0.001 mm (the resolution in X, Y, and Z axes of a CMM are 0.0001 mm. In the experimental measurement, the resolution of a CMM was rounded of the reading at the digit of 1 μm). Variations due to this finite resolution were estimated to have rectangular limits of ±0.5 μm. And the measurement was repeated five times, resulting in a maximum standard deviation of approximately 0.40 μm. Consequently, uncertainty due to limited repeatability was estimated to have a normal distribution.

Finally, the expanded uncertainty ($k = 2$) of the CMM verification along the diagonals was calculated to be $[(0.77)^2 + (0.69 \times 10^{-3}\ l)^2]^{1/2}$ μm. The uncertainty components are summarized in Table 2.

The positioning error of each diagonal of a CMM (E_x) using a step gauge is determined by replacing the l_s term of Eq. (3) with the reference length of the step gauge. As a result, the uncertainty components are evaluated as in Eq. (5).

$$u^2(E_x) = u^2(l_x) + u^2(l_s) + u^2(\delta l_{ix}) + l_N \cdot \bar{\alpha} u^2(\Delta t) \quad (5)$$

where $\bar{\alpha}$ is the average thermal expansion coefficient of the step gauge and the linear scale of a CMM, and Δt is the temperature difference between the step gauge and linear scale of a CMM. The uncertainty sources of CMM diagonal verification using a step gauge are summarized in Table 3.

5. Conclusions

A new optical measurement method to verify CMMs was proposed. It is a single-mode fiber pulsed interferometer that performs non-contact measurements on a ball lens of refractive index 2 as a target. The target can be used for absolute-length measurements in all directions. The measurement range is up to 10 m, and the proposed method is directly traced to the SI base unit. If the uncertainty due to the finite resolution of a CMM is ignored because of dependent upon machines, the measurement capability of the proposed system is approximately $[(0.36)^2 + (0.69 \times 10^{-3}\ l)^2]^{1/2}$ μm, which the coverage factor k is 2, or approximately 7 μm for the indication length of 10 m. The experimental results show that the measurement accuracy depends on noise in the interference fringe caused by airflow fluctuations and mechanical vibrations. However, measurement uncertainty is smaller than that of the artifact test method due to the effects of air temperature. In addition, the measurement time of the proposed method is 60% less than that of the artifact method because of its shorter start-up time; the proposed method can be used in measurements after a 30-min system warm-up, while the artifact method requires a waiting period of more than 3 h to achieve a stabilized gauge temperature for each alignment. Moreover, the alignment procedure is easier in the proposed system because of the compact and convenient optical components. However, the proposed method is a non-contact one, and therefore its CMM verification does not include effects of the CMM probing system.

Acknowledgements

The authors appreciate the step gauge and reference lengths provided by the National Metrology Institute of Japan (NMIJ), Lengths and Dimensions Division, for use in the measurement comparison between the proposed method and the artifact test method.

References

[1] ISO10360-2. Geometrical Product Specification (SPC). Acceptance and reverification tests for coordinate measuring machines (CMM). Part 2: CMMs used for measuring linear dimensions. International Organization for Standardization; 2009.
[2] EAL-G17. Coordinate measuring machine calibration. European Cooperation for Accreditation of Laboratories; 1995.
[3] Abbe M, Takamasu K, Ozono S. Reliability on calibration of CMM. Measurement 2003;33:359–68.
[4] Aguilar JJ, Aguado S, Santolaria, Samper D. Multilateration in volumetric verification of machine tool. In: XX IMEKO World Congress. 2012.
[5] Schwenke H, Schmitt R, Jatzkowski P, Warmann C. On-the-fly calibration of linear and rotary axes of machine tools and CMMs using tracking interferometer. CIRP Ann Manuf Technol 2009;58:477–80.
[6] Barakat NA, Elbestawi MA, Spence AD. Kinematic and geometric error compensation of a coordinate measuring machine. Int J Mach Tool Manuf 2000;40:833–50.
[7] Trapet E, Wäldele F. A reference object based method to determine the parametric error component of coordinate measuring machines and machine tools. Measurement 1991;9:17–22.
[8] Swornowski PJ. A new concept of continuous measurement and error correction in coordinate measuring technique using a PC. Measurement 2014;50:99–105.
[9] Weckenmann A, Lorz J. Monitoring coordinate measuring machine by calibrated parts. In: 7th international symposium on measurement technology and intelligent instruments. 2005. p. 183–90.
[10] Curran E, Phelen P. Quick check error verification of coordinate measuring machines. J Mater Process Technol 2004;15:5–156, 1207–13.
[11] Cauchick-Miguel P, King T, Davis J. CMM verification: a survey. Measurement 1996;17:1–16.

[12] Phillips SD, Sawyer D, Borchardt B, Ward D, Beutel DE. A novel artifact for testing large coordinate measuring machines. Precis Eng 2001;25:29–34.
[13] Arriba L, Trapet E, Bartscher M, Franke M, Balsamo A, Costelli G, et al. Method and artifacts to calibrate large CMMs. European standards measurements and testing programme, Project SMT4-PL97-2330; 1999.
[14] Cundiff ST, Ye J. Femtosecond optical frequency comb. Rev Mod Phys 2003;75:325.
[15] Matsumoto H, Wang X, Takamasu K, Aoto T. Absolute measurement of baselines up to 403 m using heterodyne temporal coherence interferometer with optical frequency comb. Appl Phys Express 2012;5:046601.
[16] Chanthawong N, Takahashi S, Takamasu K, Matsumoto H. Performance evaluation of a coordinate measuring machine's axis using a high-frequency repetition mode of a mode-locked fiber laser. Int J Precis Eng Manuf 2014;15:1507–12.
[17] Wang X, Takahashi S, Takamasu K, Matsumoto H. Spatial positioning measurements up to 150 m using temporal coherence of optical frequency comb. Precis Eng 2013;37:635–9.
[18] Wiroj S, Hirokazu M, Satoru T, Kiyoshi T. Verification of the positioning accuracy of industrial coordinate measuring machine using optical-comb pulsed interferometer with a rough metal ball target. Precis Eng 2015;41:63–7.
[19] Balling P, Křen P, Mašika P, van den Berg SA. Femtosecond frequency comb based distance measurement in air. Opt Express 2009;17:9300–13.
[20] Ciddor PE, Hill RJ. Refractive index of air. 2. Group index. Appl Opt 1999;38:1663–7.
[21] Ciddor PE. Refractive index of air: new equations for the visible and near infrared. Appl Opt 1995;35(9):1566–73.
[22] Šmíd R, Číp O, Lazar J. Precise length etalon controlled by stabilized frequency comb. Meas Sci Rev 2008;8(5):114–7.
[23] Nakamura O, Goto M, Toyoda K, Takai N, Kurosawa T, Makamata T. A laser tracking robot-performance calibration system using ball-seated bearing mechanisms and a spherically cat's-eye retroreflector. Rev Sci Instrum 1994;65:1006–11.
[24] Toshiyuki T, Mitsuo G, Sonko O, Ruimin Y, Tomizo K. Whole-viewing-angle cat's-eye retroreflector as a target of laser trackers. Meas Sci Technol 1999;10:N87–90.
[25] ISO 1. Geometrical product specification (SPC). Standard reference temperature for geometrical product specification and verification. International Organization for Standardization; 2002.
[26] Evaluation of measurement data-Guide to the expression of uncertainty in measurement, GUM 1995 with minor corrections, vol. 100, 1st Ed. JCGM; 2008.
[27] EA-4/02. Evaluation of the uncertainty of measurement in calibration. European Co-operation for Accreditation; 2013.